Gradus Vol 10, No 2 (2023)
ISSN 2064-8014

NUMERIC STRUCTURAL ANALYSIS OF HIGH COMPLEXITY STEEL FRAME STRUCTURES

Attila Piros[0000-0002-0829-8062 1*]

[1] Department of Innovative Vehicles and Materials, GAMF Faculty of Engineering and Computer Science, John von Neumann University, Hungary
https://doi.org/10.47833/2023.2.ENG.001

Keywords:
FEA simulation
Logistic system
Deformation
Geometric simplification

Article history:
Received 29 October 2022
Revised 28 April 2022
Accepted 1 June 2023

Abstract
In the case of a heavy machine, its framework contains many components. The numerical simulation of this complex structure requires serious computational background. This paper introduces the application of the top-down design methodology and geometric simplification to create a manageable computer model for FEA.

1 Introduction

There are several articles about the automatization of workshop logistic [1][2][3]. The automation procedure requires development of special machines and equipment. During the current research, a series of FEA tests were carried out, following a design of the zero-point lifting system and of the unit suitable for carrying out the cut pieces and waste of the plasma cutting equipment already built at ESZO Kft.

Products to be processed

- square and rectangular hollow sections ($20 - 250mm$)
- circular hollow sections (diameter $60 - 324mm$)
- other rolled sections: wide flange, channel, “I” “L” angle, “T” profiles ($80 - 300mm$)

These are originally 6-meter-long bars, but ESZO Kft. requests that even 1-meter-long residual materials be able to process.

For easy understanding, the structure of machine must be divided into five separate units:

1. Zero-point lifting: moving zero-point and stationery zero-point - their task is to receive the workpieces from the feeder and align them in the chuck. Zero-point lifts can be divided into two sub-units, moving and stationary zero-point lifts.
2. Feeder – its task is to feed unprocessed workpieces towards the plasma cutter at an orderly pace. The feeder works by the help of several movements closely coordinated with each other. We distinguish between 3 drives, which are as follows:
   - chain drive of a stationary feed line,
   - chain drive of a moving feed line,
   - braking mechanism.

   The gear motors responsible for drives 1 and 2 are the same.
3. Dispenser - can be divided into two parts: dispenser roller row and dispenser chuck. Its task is to retrieve the processed pieces and hand them over to the sorting bridge crane. The task of the dispenser is to take the plasma-cut workpiece, which is considered a finished product from the point of view of the entire structure, out of the cutting area and then hand it over to the sorting bridge crane. In terms of its operation, it can be divided into two parts:

* Corresponding author.
E-mail address: piros.attila@gamf.uni-neumann.hu

- Conveying roller row - which is divided into parts inside and outside the cutting area.
- Carrying out chuck – In cross-section, it grips the workpiece from all sides and can be moved in the direction of carrying out.

4. Small piece and waste conveyor - its task is to remove waste shavings and small pieces directly from the workplace. This section is mainly built from commercial components, and it has only moderate load. These are the reasons that this section is not in the scope of the paper.
5. Bridge crane - its task is to take the processed pieces from the dispenser and sort them into storage boxes. There are four different movements in the structure; 1. horizontal movement of the bridge, 2. horizontal movement of the running block, 3. vertical movement of the gripper arm, and 4. movement of the gripper claws. Two synchronized flat spur gear motors are responsible for moving the bridge crane. The bridge crane moves at a speed of $v = 0.5[m/s]$. Its range of motion depends on how many frame elements have been installed. The width of a frame is $l = 2.7[m]$. Thus, the range of motion $X = (n + 1)l[m]$ where n is the number of frames, and the plus one is needed because the part above the dispensing chuck must always be included. Radial load capacity: $6500[N]$. Two running blocks will be installed on the bridge, which does not differ from each other in any way. The blocks are moved with a rack and pinion gear connection. Bevel gear motors take care of the drive.

The positions of the workpiece are described in Figure 1.

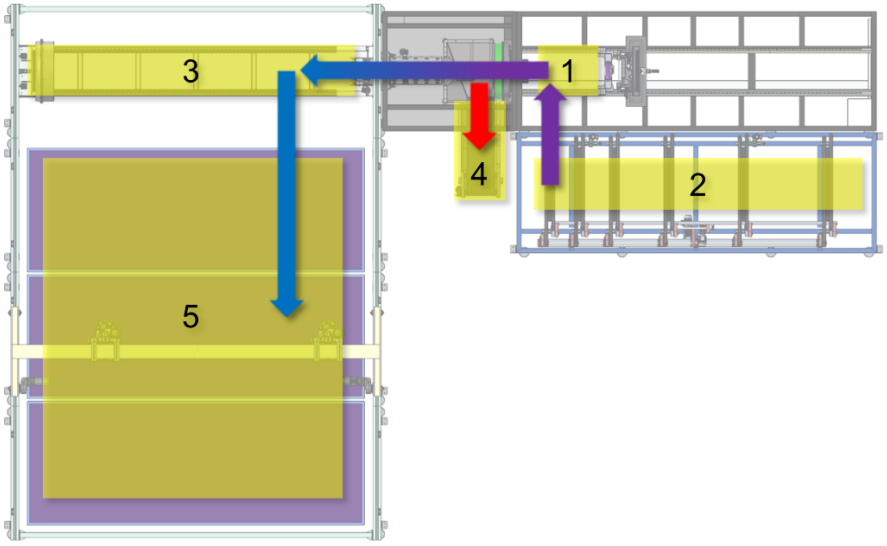

Figure 1 Workpiece positions during machining

2 Methods

The available CAD models were simplified during the project before the FEA simulations were performed. All of the materials are set to S235-JR2 concerning to the physical structure. The high number of small geometric details of the original CAD model makes the numerical analysis quite complex. Because of the results of the simulations following the preparation, further examination of the feeder levers became justified. The chapter details the above.

2.1 Preparation of CAD models for FEA simulation (pre-processing)

The FEA simulation processed with PTC Creo Simulation 4.0 was preceded by the analytical calculation of the load cases.

During finite element simulation, the models are divided into small, geometrically defined elements (mixed polinominal mesh with second order solid and shell elements), during which they are connected only at their nodes.

Performing significant geometric simplifications on the available CAD models, as well as excluding components that do not affect the force flow occurring in the structure during loading (e.g., chuck, drive system elements) from the assembly, are part of the pre-processing process of the finite element simulation [4]. The preparation also includes the definition of loads and boundary conditions, as well as meshing with solid and shell elements.

2.1.1 Zero-point lifting system preparation

The moving and stationary hoists of the hoisting system transfer the load to the frame structure on the sliding rails, thus when examining the frame structure, the models of the hoists can be replaced with the loads on the rails.

After excluding the lifters, fasteners, and elements responsible for movement from the assembly, CAD geometries were simplified by removing rounds, chamfers, and holes [5]. The simplified geometries of the building elements of the frame structure can be replaced by surface pairs (Shell Pair), thus creating shell models. After simplifying the geometries and creating shell models, the loads and boundary conditions were defined.

Weight of biggest profile (HEB300): $m = 702kg$ → Highest load: $G = 6886.62N$.

Taken loads:

$F1: 3443N$ (half of largest profile load),

$F2: 1722N$ (a quarter of largest profile load per rail),

$F3: 1000N$(overestimated load of clamping chuck and sliding system).

2.1.2 Feeding system preparation

After excluding the elements responsible for movement from the assembly, CAD geometries were simplified and replaced by surface pairs (Shell Pair), thus creating shell models.

Weight of biggest profile (HEB300): $m = 702kg$ → Highest load: $G = 6886.62N$.

Taken loads:

$F1: 1755N$(based on results of previous FEA simulation),

$F2: 1722N$(1/6 of twice the maximum profile load per feeding arm).

Figure 2 describes the simulation result obtained at the project's completion, showing deformation of $14.14mm$. The FEA calculation based on single pass adaptive method to ensure the mesh independency.

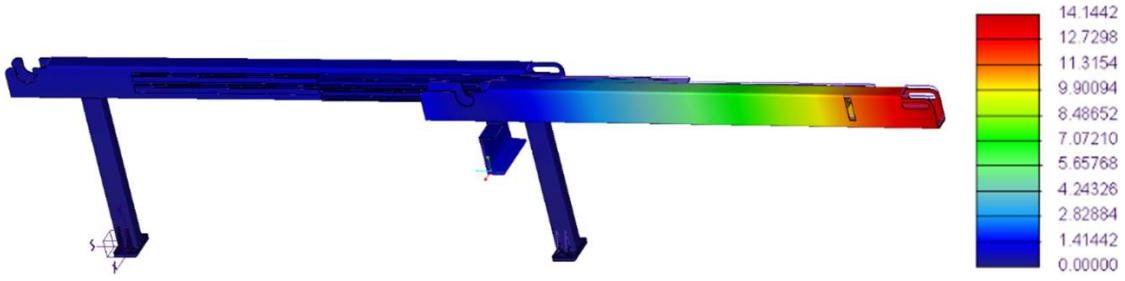

Figure 2 Feed arm deformation [mm]

In addition to this result, it can also be seen from Figure 3 that a rail system that differs excessively from reality was created for the simulation. This is because, for example, the rolling elements were omitted from the system. The rail created during the geometric simplification already has a connection, but this solution turned out to be too rigid.

Figure 3 Original and simplified rail system cross-section

With the simplified rail system, the degree of deformation is approximately one-tenth of the result of the original simulation. Due to the significant deviation, additional simulations were run without geometry simplification to verify the initial results. Balls providing power transmission were missing from the model of the original rail system, so they were replaced in several ways with solid rods and tubes with wall thicknesses of 2 and $1mm$ (Figure 4).

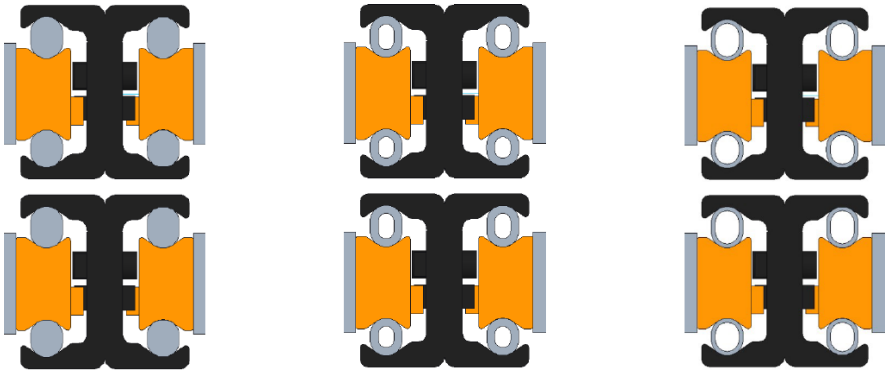

Figure 4 Rail systems supplemented with solid rods and 2 and 1 mm tubes

2.1.3 Dispensing system preparation

The moving delivery chuck of the dispensing system transfers the load to the frame structure on the sliding rails, and the dispensing roller row is partly attached to the side of the plasma cutter and partly to the frame structure, thus when examining the frame structure, the former models can be replaced with the loads on the rails and frame structure.

After excluding the chuck, roller row, fasteners, and elements responsible for movement from the assembly, CAD geometries were simplified by removing rounds, chamfers, and holes. The simplified geometries of the building elements of the frame structure can be replaced by surface pairs (Shell Pair), thus creating shell models.

After simplifying the geometries and creating shell models, the loads and boundary conditions were defined.

Weight of biggest profile (HEB300): $m = 702kg$ → Highest load: $G = 6886.62N$.

Taken loads:

$F1: 4940N$ (half of largest profile load + roller row load),

$F2: 1722N$ (a quarter of largest profile load per rail),

$F3: 1000N$ (overestimated load of clamping chuck and sliding system).

2.1.4 Bridge crane system preparation

The gripping claws of the bridge crane system transfer the load to the moving arms, thus when examining the frame structure, the former models can be replaced with the loads on the point of attack.

After excluding the gripping claws, fasteners, and elements responsible for movement from the assembly, CAD geometries were simplified by removing rounds, chamfers, and holes.

The simplified geometries of the building elements of the frame structure can be replaced by surface pairs (Shell Pair), thus creating shell models.

After simplifying the geometries and creating shell models, the loads and boundary conditions were defined.

Weight of biggest profile (HEB300): $m = 702kg$ → Highest load: $G = 6886.62N$.

Taken loads:

$F1: 3443N$ (half of largest profile load),

$F2: 87.5N$ (calculated load resulting from kinetic energy in the event of a collision).

Figure 5 shows a simplified model of the bridge crane with fixed lower beams.

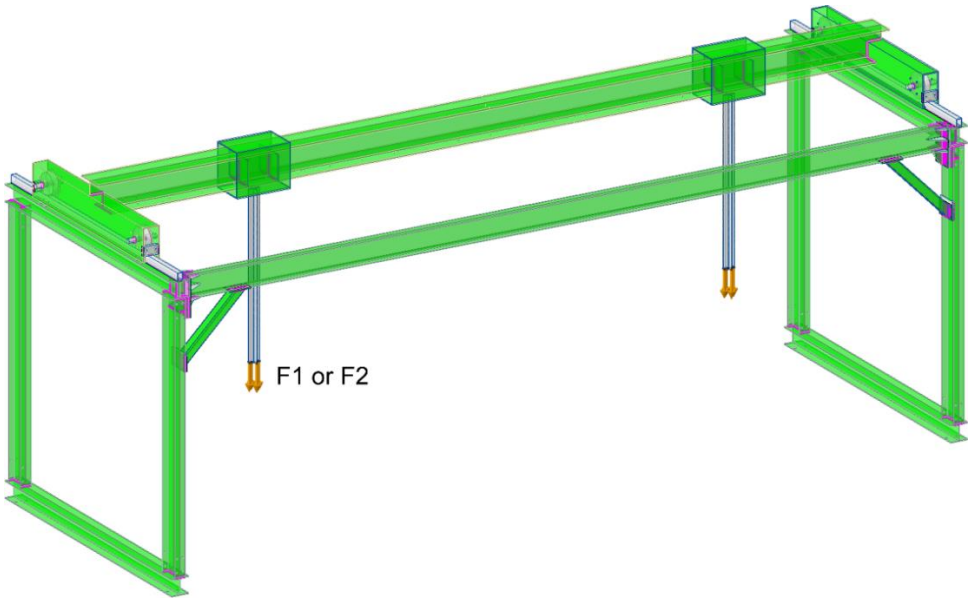

Figure 5 A simplified model of a bridge crane with shell elements and loads

3 Results

3.1 Evaluation of FEA simulations (post-processing)

After running the simulations, the results can be evaluated. For the four sub-assemblies, it can be uniformly observed that the critical stress is always below the limit value. For material handling structures, the degree of deformation is significant.

3.1.1 Zero-point lifting system simulation results

At its maximum load, the most considerable deformation value is $0.02mm$, which can be calculated in the form of deflection at the stationary zero-point lift.

At its maximum load, the highest stress value is $25.7MPa$, which can be calculated at the stationary zero-point lifter.

3.1.2 Feeding system simulation results

At the maximum load of a section, the value of the most significant deformation is $1.26mm$, which can be calculated in the form of bending at the end of the feeding arms.

At the maximum load of a section, the maximum stress value is $55.4MPa$, which can be calculated in the middle of the sliding rail system.

3.1.3 Dispensing system simulation results

At its maximum load, the value of the most considerable deformation is $0.04mm$, which can be calculated in the form of bending at the dispensing roller row.

At its maximum load, the maximum stress value is $99.4MPa$, which can be calculated at the dispensing roller row.

3.1.4 Bridge crane system simulation results

At maximum tensile stress, the most considerable deformation value is $0.43mm$, which can be calculated in the form of bending and stretching in the middle of the crane and at the end of the moving arms.

If the crane hits a stationary object during movement, the maximum deformation value at the maximum tensile and twisting stress is $1.19mm$, which can be measured at the end of the moving arms in the form of twisting.

At maximum tensile stress, the maximum stress value is $83.85MPa$, and at maximum tensile and twisting stress, it is $115.4MPa$, which can be measured at the connection of the running blocks and moving arms.

3.1.5 Stresses and deformations

The final results of these analyses reflect reasonable values both in deformation and Von Mises equivalent stress (Table1). The low values geometric deformation enable to design a reliable control system.

Table 1 Maximum deformations [mm] and stresses [MPa]

	1. Zero-point lifting system	***2. Feeding system***	***3. Dispensing system***	***4. Bridge crane system***
Maximum deformation [mm]	0.02	1.26	0.04	0.43
Maximum stress [MPa]	25.7	55.4	99.4	115.4

4 Conclusion

Although nowadays the computational capacity is continuously increasing, but the numerical simulation of large machines generates serious challenges for mechanical engineers. Application of simplified CAD geometries makes the calculation procedure much easier but it has some possible errors, as well. During the simulations performed with the original models, instead of the $14.14mm$ deformation, $7.72mm$, $7.95mm$, and $8.45mm$ deformation occurred (Figure 6), which indicates that the rail system suffers a significant part of the deflection of the entire system, therefore, the judicious selection of their type is crucial for the system's overall functioning.

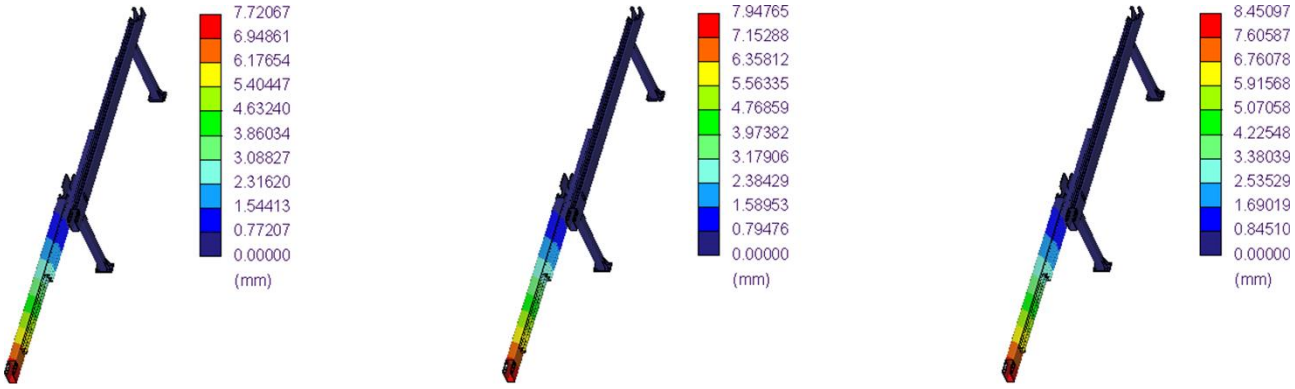

Figure 6 Deformation results of rail systems [mm]

Acknowledgment

ESZO Kft.'s application for support under the Economic Development and Innovation Operative Program of GINOP registered with the identification number 2.1.7-15-2016-00764 was considered worthy of approval. Within the framework of the project, the company developed and then manufactured the pipe holder product family with the EMARUG name.

References

[1] Ece Yağmur, Saadettin Erhan Kesen: A memetic algorithm for joint production and distribution scheduling with due dates, Computers & Industrial Engineering, 2020, Vol. 142, 106342, DOI: 10.1016/j.cie.2020.106342
[2] Yushuang Hou, Yaping Fu, Kaizhou Gao, Hui Zhang, Ali Sadollah: Modelling and optimization of integrated distributed flow shop scheduling and distribution problems with time windows, Expert Systems with Applications, 2022, Vol. 187, 115827, DOI: 10.1016/j.eswa.2021.115827
[3] Salih Duffuaa, Ahmet Kolus, Umar Al-Turki, Ahmed El-Khalifa: An integrated model of production scheduling, maintenance and quality for a single machine, Computers & Industrial Engineering, 2020, Vol. 142, 106239, DOI: 10.1016/j.cie.2019.106239
[4] Foucault, G., Cuillière, J.C., François, V., Léon, J.C. and Maranzana, R.: Adaptation of CAD model topology for finite element analysis, Computer-Aided Design, 2008, Vol. 40, No. 2, pp. 176-196, DOI: 10.1016/j.cad.2007.10.009
[5] Atul Thakur, Ashis Gopal Banerjee, Satyandra K. Gupta: A survey of CAD model simplification techniques for physics-based simulation applications, Computer-Aided Design, 2009, Vol. 41, Issue 2, pp. 65-80, DOI: 10.1016/j.cad.2008.11.009